# Graphic Abstract

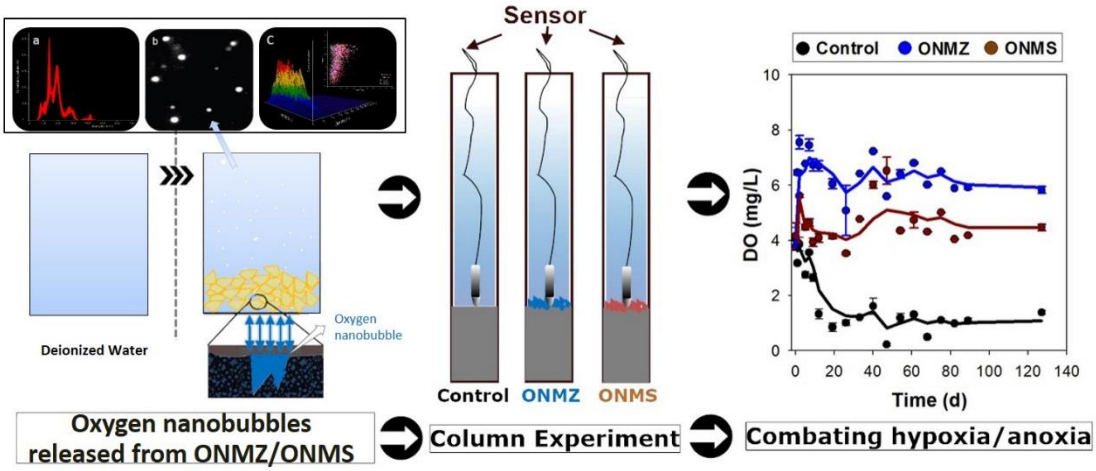


# Highlights

- Oxygen nanobubble is a potentially promising technique to mitigate hypoxia/anoxia
- Oxygen nanobubble modified zeolite can effectively deliver oxygen to bottom water
- The oxygen-locking surface sediment layer is crucial in reducing sediment anoxia
- Oxygen-locking sediment layer can switch the anoxia sediment from P source to sink

# Combating hypoxia/anoxia at sediment-water interfaces: a preliminary study of oxygen nanobubble modified clay materials

Honggang Zhang[1], Tao Lyu[2], Lei Bi[1], Grant Tempero[3], David P. Hamilton[3], Gang Pan[*1,2]

[1]*Research Center for Eco-Environmental Sciences, Chinese Academy of Sciences, Beijing 100085, China*

[2]*School of Animal, Rural and Environmental Sciences, Nottingham Trent University, Brackenhurst Campus, NG250QF, UK*

[3]*School of Science, University of Waikato, Private Bag 3105, Hamilton 3240, New Zealand*

[*]Corresponding author: gpan@rcees.ac.cn (GP)

## Abstract

Combating hypoxia/anoxia is an increasingly common need for restoring natural waters suffering from eutrophication. The oxygen nanobubble modified natural particles were investigated for mitigating hypoxia/anoxia at sediment-water interfaces (SWI) in a simulated column experiment. By adding oxygen nanobubble modified zeolites (ONMZ) and local soils (ONMS), the oxygen nanobubble concentrations ($10^5$-$10^7$ particles/mL) were several orders of magnitude higher in the water than the original water solution ($10^4$ particles/mL) within 24 hours. In the column experiment, an oxygen-locking surface sediment layer were formed after capping with ONMZ and ONMS particles. The synergy of diffusion of oxygen nanobubbles and retention of oxygen in this layer contributes to both the increase of DO and reversal of hypoxic conditions. The overlaying water maintained significantly higher dissolved oxygen (DO) values (4-7.5 mg/L) over the experimental

period of 127 days in ONMZ and ONMS compared with the control systems (around 1 mg/L). Moreover, the oxidation-reduction potential (ORP) was reversed from -200 mV to 180-210 mV and maintained positive values for 89 days in ONMZ systems. In the control systems, ORP was consistently negative and decreased from -200 mV to -350 mV. The total phosphorus (TP) flux from sediment to water across SWI was negative in the ONMZ and ONMS treated systems, but positive in the control system, indicating the sediment could be switched from TP source to sink. The oxygen-locking capping layer was crucial in preventing oxygen consumption caused by the reduced substances released from the anoxic sediment. The study outlines a potentially promising technology for mitigating sediment anoxia and controlling nutrients release from sediments, which could contribute significantly to addressing eutrophication and ecological restoration.

**Keywords:** deep water, eutrophication control, harmful algae blooms, nutrient flux, oxygen deliver

## 1. Introduction

Hypoxia/anoxia is a global threat to aquatic ecosystems, often inducing "dead zones" at the sediment-water interface (SWI) (Diaz and Rosenberg, 2008; Feist et al., 2016; Stramma et al., 2008). In the dead zones, sediment release rates may be accelerated for many constituents, including phosphorus, nitrogen, iron, manganese, methyl-mercury and hydrogen sulfide (Beutel et al., 2008; De Vittor et al., 2016; Gantzer et al., 2009; Testa and Kemp, 2012; Zhu et al., 2013). Among the released substances, phosphorus and nitrogen can lead to eutrophication, which is often associated with harmful algal blooms (Funkey et al., 2014). Moreover, the hypoxic/anoxic condition can be exacerbated by the additional oxygen demand from the mineralization of dead algal biomass (Diaz

and Rosenberg, 2008; Testa and Kemp, 2012). Thus, mitigation of hypoxia/anoxia at the SWI is crucial for both water quality improvement and eutrophication control.

Current efforts de-signed to replenish benthic dissolved oxygen (DO) and remove the anoxic environment are often based on the directly injecting either air (aeration) (Henares et al., 2015), or oxygen gas (oxygenation) (Bierlein et al., 2017) sometimes using oxygen-supersaturated water (Forth et al., 2015) into the hypoxic region near the SWI. Although these techniques have been reported to be effective to some extent, they are still limited by high cost and efficiency at large scale (Bormans et al., 2016). Additionally, gas or water pumped into the SWI region may disturb the settled sediment and induce internal releases of nutrients and other contaminants to the water column, as well as potentially leading to additional oxygen consumption and increase hypoxia (Bierlein et al., 2017). The pump system also needs to be continuously operated to maintain the oxygen supply to the SWI, otherwise DO may be rapidly consumed, leading to rapid return of anoxia (Bryant et al., 2010). In the Baltic Sea, where hypoxic waters have expanded in area from 5,000 to > 60,000 $km^2$ in the last century (Carstensen et al., 2014), enhanced ventilation of deep waters through additional input of oxygenated surface water has been suggested (Conley et al., 2009). However, this method will require > 30 years to take effect and may cause a drastic change in stratification and alteration of the biodiversity (Funkey et al., 2014). Ventilation by pumping oxygen-rich water downward to alleviate hypoxia in the Baltic Sea is estimated to require more than 100 pump stations (0.6 MW each) at a cost of around 20,000 million Euros (Stigebrandt and Gustafsson, 2007). Therefore, developing a more cost-effective and sustainable technique for hypoxia/anoxia mitigation in bottom waters and at the SWI is vitally important.

Oxygen nanobubbles have attracted increasing attention in recent years due to the characteristics of high gas solubility and long lifetime of oxygen in the liquid (Ebina et al., 2013; Peng et al., 2015). As opposed to oxygen gas (Cavalli et al., 2009), nano-scale oxygen bubbles could slowly diffuse oxygen into the surrounding water phase and last more than 70 days when diameter is <200 nm (Ebina et al., 2013). The oxygen nanobubble technique has already been widely used in medicine (Cai et al., 2015), physiology (Ebina et al., 2013) and water treatment (Agarwal et al., 2011). However, a cost-effective method to deliver the oxygen nanobubble into SWI for hypoxia/anoxia mitigation remains a bottleneck. It was recently reported that oxygen nanobubbles can be generated and persist at solid particle-water interfaces (i.e., surface nanobubbles) (Pan et al., 2016; Wang et al., 2016; Yang et al., 2013). The presence of oxygen nanobubbles has been proven and quantified at the rough and irregular surfaces of clay particles (Pan et al., 2016). It is a means to increase total oxygen content in a suspension by adding clay particles loading with oxygen nanobubbles (Pan and Yang, 2012; Pan et al., 2011). Sedimentation of a carrier loaded with oxygen nanobubbles due to the gravity effect provides a mechanism to alter the hypoxia/anoxia near the SWI but has not been investigated systematically.

Many geo-engineering methods, such as adding phosphorus-adsorbing materials, have been demonstrated to significantly contribute to remediating eutrophication control and contributing to lake restoration (Huser et al., 2016; Noyma et al., 2016; Spears et al., 2014; Waajen et al., 2016). However, the sinking materials cover the sediment and their effect on redox potential at the SWI may be temporary (Pan et al., 2012). Additionally, most of the adsorbing materials, e.g., metal salts and Phoslock®, are synthesized artificially and may have potential side-effects on the environment. Natural sediments entering lakes through weathering and runoff, have high microporous surface area

(Pan et al., 2013). These natural particles have potentially as oxygen nanobubble carriers to deliver oxygen to the SWI. However, no previous study has applied such technology and there is little knowledge about the effects of oxygen nanobubbles on the oxygen conditions, redox potential and nutrient fluxes at the SWI.

The objective of this study is to investigate for the first time the efficacy and sustainability of a surface oxygen nanobubble technique for mitigating hypoxia/anoxia and its effect on nutrient fluxes across the SWI. Local soil and natural zeolite were selected as the oxygen nanobubble carriers in the experiment. After oxygen nanobubble modified zeolite (ONMZ) or oxygen nanobubble modified soils (ONMS) were applied in simulated eutrophic water-sediment systems in the laboratory columns, oxygen levels in the overlying water and redox potential at SWI were monitored. Nutrient concentrations, including total phosphorus (TP), total nitrogen (TN), ammonium ($NH_4^+$-N), nitrate ($NO_3^-$-N), and nitrite ($NO_2^-$-N), were measured in the overlying water and nutrient fluxes across the SWI were calculated.

## 2. Materials and methods

### 2.1 Preparation of oxygen nanobubble modified materials

Natural zeolite and local soil were selected as the carrier materials to investigate the effect of surface oxygen nanobubble technology on hypoxia/anoxia mitigation at the SWI. Zeolite with particle size of 1-2 mm was purchased from Yongjia Natural Minerals Ltd., Hebei, China. Local soil from Lake Ngaroto, Waikato, New Zealand, was sieved through a mesh sieve to remove particles >380 μm. Ngaroto is the largest peat lake in Waikato region, with a surface area of about 108 ha, maximum depth of 4 m and average depth of c. 2 m. Land in the catchment of this lake is mostly used for pastoral

grazing. The lake is hypertrophic and has major cyanobacteria harmful algal blooms throughout summer. The specific surface area and micropore size of the natural zeolite and local soil were determined by the Brunauer–Emmett–Teller (BET) method with a Micromeritrics ASAP-2020 apparatus (Micromeritics Inc., USA) (Zhang et al., 2014).

The zeolite and soil, were washed with deionized water and dried for 10 h at 90 °C. The preparation of oxygen nanobubble modified zeolite (ONMZ) and soil (ONMS) followed a modified method based on exposure to oxygen supersaturating ambient conditions (Pan et al., 2016). Briefly, the materials (zeolite or soil) were placed into a pressure-resistant and airtight container. A vacuum was created to hold pressure to -0.08 to -0.1 MPa for 2 h to remove gas from the micropores of zeolite and soil. Thereafter, pure $O_2$ (99.99%) was pumped into the container and held at a pressure of 0.12 to 0.15 MPa for 4 h to load the $O_2$. The oxygen nanobubble loading process, including the creation of the vacuum, was repeated three times to achieve supersaturation of $O_2$ in the particle micropores.

**2.2 Nanobubbles analysis**

Prior to the column experiment, the release potential of oxygen nanobubbles into water from the modified solid particles was tested via a flask experiment. Twenty grams of the oxygen nanobubble modified zeolite or soil was put into 250 mL flasks with 200 mL deionized water and sealed by gas-permeable sealing film (0.3 μm). Controls consisted of flasks of 250 mL filled with 200 mL of deionized water. Each control and treatment flask experiment were conducted in triplicate. To confirm the sequential changes of nanobubble release, size (detection range; 10-1000 nm) and concentration of oxygen nanobubbles, measurements were conducted at 1 min, 6 h and 24 h in a nanoparticle-tracking analysis instrument (NanoSight NS500 & NTA 2.0 Analytical Software,

Malvern Instrument Ltd, Salisbury, UK) at room temperature (24 ± 1$^{o}$C).

### 2.3 Column experiment

The column experiment was conducted in an indoor laboratory in University of Waikato, New Zealand, over a total duration of 127 days. Six plexiglass cylinders with identical inner diameter of 12 cm and height of 150 cm were used as incubation columns (Fig. S1**Error! Reference source not found.**). Each column was filled in the bottom 20 cm with the lake sediment and with filtered (mesh size of 25 μm) lake water (also from Lake Ngaroto) to a height of 120 cm. Each experimental column was wrapped with black plastic to shield the system from ambient light. The columns included duplicates of a control, treatment by oxygen nanobubble modified natural zeolite (ONMZ) and oxygen nanobubble modified local soil (ONMS). The oxidation-reduction potential (ORP) meter (HANNA, HI2001) was placed lightly on the sediment surface in each column to monitor the change of ORP at the SWI throughout the experiment. After a 3-day stabilization period, the ONMZ and ONMS treatment systems were pretreated by flocculation using 3 mg/L chitosan modified soils (Li and Pan, 2013) following by application of approximately 100 g of ONMZ and ONMS, resulting a 2 cm depth capping layer.

### 2.4 Sampling and analysis

During the experiment, overlying water samples (100 mL) from each column were carefully collected from 5 cm above the sediment using a syringe with a siphon. The collected water samples were evenly separated into three parts (c.33 mL) which were measured for turbidity and nutrient concentrations (TP, TN, $NH_4^+$-N, $NO_3^-$-N, and $NO_2^-$-N). After each sample collection, all columns were slowly replenished with the original filtered lake water to compensate for the sampling losses.

147 Turbidity was analyzed with portable turbidity meter (HANNA, HI98713). TP was determined using
148 a potassium persulfate digestion-Mo-Sb-Vc colorimetric method, TN using an alkaline potassium
149 persulphate digestion−ultraviolet spectrometer, $NH_4^+$-N with Nessler's colorimetric, and $NO_3^-$-N and
150 $NO_2^-$-N with ultraviolet colorimetric method with and without cadmium column reduction,
151 respectively (APHA, 1998). The DO was measured using a Yellow Springs Instruments (YSI, Proplus)
152 by carefully putting the meters into the overlying water and holding at 1-2 cm above the SWI. To
153 avoid cross contamination, the meters were carefully cleaned with Milli-Q water and ethanol between
154 measurements. The DO and turbidity were measured simultaneously with ORP from the in-site meters
155 (HANNA, HI2001) at days 0, 1, 2, 5, 7, 9, 12 and then every around 7 days until day 89, although
156 DO was measured until day 127. The concentrations of TP, TN, $NH_4^+$-N, $NO_3^-$-N, and $NO_2^-$-N were
157 measured at 7-day frequency until 47 days and then monitored every 14 days. The nutrient fluxes
158 were calculated from day 19 in order to minimize the influence caused by suspended substances
159 sedimentation as indicated by relative low turbidity in control. All samples were tested in triplicate
160 for each duplicate column, values were averaged and standard deviations for the samples from the
161 same treatment system.

162 **2.5 Calculation**

163 The monitoring data on nutrient concentrations obtained after day 19 was used to calculate
164 nutrient fluxes at the SWI. The average nutrient flux was calculated according to the following mass
165 balance Equation (1):

166 $$F_n = \frac{[V(c_n - c_m) + \sum_{j=1,i=1}^{n} V_j(c_n - c_i)]}{S \times t} \quad (1)$$

167 Where $F_n$ is the flux on $n^{th}$ sampling day ($mgm^{-2}d^{-1}$), $V$ is the volume of overlying water (L), $c_n$ is the nutrient

concentration ($mgL^{-1}$) on $n^{th}$ sampling day (n>19), $c_m$ is the nutrient concentration ($mgL^{-1}$) on $m^{th}$ sampling day when turbidity had stabilized in the three columns (i.e., the $19^{th}$ day in this study), $c_i$ is the nutrient concentration of the compensating water for maintaining the volume of water in the columns ($mgL^{-1}$), $V_j$ is volume of sampling water (L), $S$ is the cross section area of each column ($m^2$) and $t$ is incubation time (d).

### 2.6 Statistical Analysis

Sigmaplot software (version 12.5, Sigma, Inc.) and SPSS16.0 (Statistical Program for Social Sciences) were used for plotting and data analyses, respectively. A one-way ANOVA and post hoc Tukey's HSD test were used to compare water quality parameters (DO, ORP and turbidity) and nutrient concentrations between different treatment systems (control, ONMZ and ONMS) at each corresponding sampling point, with differences accepted at a significance level <0.05. To fully understand the effect of surface oxygen nanobubble technology on the hypoxia/anoxia mitigation in the column experiment, principal component analysis (PCA) was used to provide an overview of the system performance using a visualization method to normalize all parameters. PCA was used to identify different performance patterns between control, ONMZ and ONMS treatment systems during from day 19 to day 89 of the experiment. PCA was conducted using all measured parameters, including DO, ORP, turbidity, TP, TN, $NH_4^+$-N, $NO_3^-$-N and $NO_2^-$-N. The data was standardized (to a Z score with a mean = 0 and S.D. = 1) to ensure that each variable had the same influence in the analysis. Multiple correlation analysis was carried out to assess the relationships between all measured parameters in the column experiment. The data was checked for normality and homogeneity of variance prior to all statistical analysis. If variables were not normally distributed, they were log-transformed.

# 3. Results

## 3.1 Release of oxygen nanobubbles from ONMZ and ONMS

In order to verify the release of oxygen nanobubbles from the modified particles, the water solution in the flask experiment after ONMZ and ONMS addition was analyzed in a nanoparticle-tracking analysis instrument to detect the concentration and size of the nanobubbles. The concentrations of nanobubbles were both around $10^7$ particles/mL immediately after the addition (1 min) of ONMZ (Fig. 1) and ONMS (Fig. 2) into the water, and approximately 70% of the released nanobubbles were <200 nm in diameter. The concentration of nanobubbles in the water with ONMZ addition was maximal at 24 h (still around $10^7$ particles/mL), and the concentration in the water with ONMS addition decreased to $10^5$ particles/mL. Nevertheless, the concentrations were clearly elevated compared with the original deionized water, which remained around $10^4$ particles/mL (Fig. S2). The peaks in the concentration vs. size graph (Fig. 1) move toward the right direction of the x axis, which indicates that the size of nanobubbles gradually increased along with the culture time in both ONMZ and ONMS (Fig. 2) treated water. The 3D graph shows two distinct nanobubble populations, clearly confirmed by the higher light scattering intensity of the nanobubbles in ONMZ treated water compared to the ONMS treated water.

## 3.2 DO and ORP dynamics at the sediment-water interfaces

At the beginning of the column experiment, the DO and ORP of the overlying water in all systems were around 4 mg/L (Fig. 3a) and -200 mV (Fig. 3b), respectively. After the oxygen nanobubble modified particles application, DO increased in the first 5 days and reached around 7.5 and 5.5 mg/L in ONMZ and ONMS systems, respectively. Concentrations gradually decreased to 6 and 4.3 mg/L and generally remained around this level until the conclusion of the experiment on day

127 in the ONMZ and ONMS systems, respectively. However, the control system maintained a hypoxic condition with DO declining to 1 mg/L at day 20 of the experiment, and remaining around this level throughout the tested period of 127 days. Significant differences of DO concentrations in the overlaying water between each system were observed ($P<0.05$) and followed the order of ONMZ > ONMS > control (**Error! Reference source not found.**3a). ORP values showed a similar pattern as DO with significantly higher values in ONMZ, followed by ONMS and control systems along the experiment (**Error! Reference source not found.**3b). ORP values were increased from -200 mV to 210 and 180 mV in the ONMZ and ONMS systems, respectively, in the first 5 days. During the experiment, ORP decreased until day 20 and remained reasonably stable at 150 mV and -160 mV in the ONMZ and ONMS columns, respectively, until day 89. In the control columns, the ORP showed a continuous decrease from -200 mV to -350 mV by day 89.

### 3.3 Nutrient dynamics in bottom water

After 19 days of the experimental set-up, the turbidity of the overlying waters had decreased from 40 NTU to around 5 NTU in the control columns and < 1 NTU in ONMZ and ONMS treated systems (**Error! Reference source not found.**4a). Turbidity remained around this level until day 89. The control systems had elevated TP until day 50 and significantly higher TP concentrations (0.08 mg/L) in the overlying water compared with the ONMZ and ONMS treated systems (Fig. 4b). The TP concentrations in the ONMZ and ONMS treated columns maintained below 0.02 mg/L and did not show significant differences between the two treatments.

TN concentrations in the ONMS columns increased slightly and the values (around 2 mg/L) become significantly higher than those in ONMZ columns (around 1.5 mg/L) and in the control

columns (around 1.2 mg/L) at day 89 (**Error! Reference source not found.**4c). $NH_4^+$-N concentrations showed a similar tendency of increase from day 19, with the highest concentration at day 40; concentrations were around 0.1, 0.3 and 0.65 mg/L in ONMZ, ONMS and control systems, respectively (**Error! Reference source not found.**4d). Concentrations of $NH_4^+$-N gradually decreased to <0.02, 0.18 and 0.13 mg/L by day 89 in ONMZ, ONMS and control systems, respectively. The concentrations of $NO_3^-$-N (**Error! Reference source not found.**5e) and $NO_2^-$-N (**Error! Reference source not found.**4f) were significantly higher in the ONMZ and ONMS systems than that in control after 19 days of incubation. However, the concentrations in ONMZ and ONMS systems showed a clear decreasing tendency after day 80 and became similar to levels in the control systems (0.01 mg/L of $NO_3^-$-N and 0.03 mg/L of $NO_2^-$-N).

### 3.4 Nutrients fluxes across the sediment-water interfaces

Fig. 5 shows the nutrient (TP, TN, $NH_4^+$-N, $NO_3^-$-N, and $NO_2^-$-N) fluxes across from the sediment to the overlying water (effluxes) from day 26 calculated by Equation (1). The flux of TP were negative in ONMZ and ONMS systems (-0.1 to -2.3 mg/m$^2$/d). The control system had positive values of TP flux, with a decreasing tendency through time and around 0.3 mg/m$^2$/d at day 89 (**Error! Reference source not found.**5a).

Generally, flux of TN was negative (average of -10 mg/m$^2$/d) in the control during the experiment (**Error! Reference source not found.**5b), while values in the ONMZ systems were generally positive (average of 5 mg/m$^2$/d). In ONMS systems, TN flux reversed from negative to positive at day 47 and finally reached around 0 at day 89. The $NH_4^+$-N flux was positive (5-20 mg/m$^2$/d) in all systems (**Error! Reference source not found.**5c) at day 26, however, the values

declined with time, and reached around 3 mg/$m^2$/d in the control system and -1 and -4 mg/$m^2$/d in the ONMZ and ONMS systems at day 89. **Error! Reference source not found.**5d shows that the flux of $NO_3^-$-N in the ONMZ and ONMS systems was consistently positive (4-15 mg/$m^2$/d). However, the flux of $NO_3^-$-N in the control systems was always negative (< -0.8mg/$m^2$/d). The flux of $NO_2^-$-N was around 0 in the control system, however, values reversed from positive to negative in the ONMZ and ONMS systems at day 89 (**Error! Reference source not found.**5e).

### 3.5 Environmental factors identified with statistical analysis

Water quality parameters (DO, ORP and turbidity) and nutrient concentrations (TP, TN, $NH_4^+$-N, $NO_3^-$-N and $NO_2^-$-N) in the overlying water were analysed with principal component analysis (PCA) to examine differences between treatment systems (control, ONMZ and ONMS) and sampling times from day 19 to day 89 (**Error! Reference source not found.**6). The eigenvalues of all the components of the PCA are shown in Table S1. The first two components (PC 1 and PC 2) contribute high proportions (57.6% and 17.7%) of the variance in both experimental phases, thus, they were extracted as principal components for further analysis. Clear group differences between three systems were shown in the visualized figures (**Error! Reference source not found.**6), suggesting performances differed by treatment. The control systems tended to locate to the left side of the ordination, and the ONMS and ONMZ systems located in the upper right lower right side, respectively. TP and turbidity contribute substantially to the control system performance patterns due to higher levels of TP and turbidity in overlying water of the control systems. DO and ORP contribute more to the positive side of PC1 (the location of the ONMS and ONMZ systems), which means the oxygen nanobubble modified particle application reduced hypoxia/anoxia at the SWI. The DO, ORP and $NO_3^-$-N loading factors were higher for the ONMZ than the ONMS system but this was reversed for TN,

276 $NH_4^+$-N and $NO_2^-$-N.

277 Multiple correlation analysis was carried out as a blind test by homogenizing all the data from
278 all columns to assess the relationships between all the parameters (Table 1). The DO and ORP showed
279 a significant negative correlation with TP concentrations and significant positive correlation with
280 $NO_3^-$-N concentrations. TP concentrations were also negatively correlated with TN and positively
281 correlated with turbidity.

282 # 4. Discussion

283 ## 4.1 Instant increase of DO by oxygen nanobubble delivery

284 Bottom water oxygenation is an increasingly common lake management strategy for mitigating
285 hypoxia/anoxia and associated deleterious effects on water quality in deep lakes and reservoirs
286 (Bierlein et al., 2017). The current methods may require a number of large pumps with very high
287 costs and energy consumption (Funkey et al., 2014; Stigebrandt and Gustafsson, 2007). In the present
288 study, surface oxygen nanobubble technology was demonstrated to deliver oxygen into the water or
289 to the SWI using a carrier of modified zeolite (ONMZ) or soils (ONMS) through gravity settling with
290 minimum energy consumption. During the ONMZ and ONMS treatments, part of the oxygen loaded
291 on the microporous surfaces of zeolite and soil quickly diffused into water through both visible
292 microbubbles (Fig. S3) and non-visible oxygen nanobubbles (Fig. 1 and 2), and instantly increased
293 the DO concentrations from 4 mg/L to 7.5 and 5.5 mg/L in ONMZ and ONMS treated systems,
294 respectively, in the first 5 days (**Error! Reference source not found.**3a). Oxygen nanobubbles were
295 directly detected in the water through the flask experiment, which verified that they could be
296 generated/delivered and then released to the surrounding bulk water from the ONMZ and ONMS

297 (**Error! Reference source not found.**. 1 and 2). The formed oxygen-locking sediment capping layer
298 not only released oxygen into the water, but also retained oxygen which could significantly mitigate
299 and even reverse the anoxic condition at the sediment-water interfaces (Fig. 3b). Currently,
300 hypolimnetic oxygenation need to develop some novel oxygen diffuser equipment in order to prevent
301 any sediment resuspension (Gafsi et al., 2016). The settling delivery method via clay or soil particle
302 carriers can fundamentally avoid the typical problems of resuspension of sediment and rigorous
303 turbulence to the SWI faced by conventional deep water aeration methods, which may be important
304 for lake restoration in maintaining natural stratification conditions (Beutel and Horne, 1999; Gachter
305 and Wehrli, 1998). The ONMZ was more efficient in supplying oxygen to the SWI than the ONMS,
306 which may due to the locking ability of oxygen by zeolite particles as well as its larger
307 specific surface area than the natural local soils (Table S2).

308 **4.2 Sustained reversal of hypoxia/anoxia at the SWI**

309 The enhanced DO levels in bottom water resulting from oxygenation by conventional pumping
310 methods may be rapidly negated after turning the pump off (Bierlein et al., 2017; Bryant et al., 2010;
311 Gachter and Wehrli, 1998). Rapid depletion of DO occurs through oxidation of both organic detritus
312 and reduced chemical substances from the sediment and thus restoration of oxygenation is a long-
313 lasting project (Liboriussen et al., 2009). The maintenance of higher DO levels in the ONMZ and
314 ONMS treated systems in the present study can be attributed to the long lifespan of the oxygen
315 nanobubbles and oxygen retention within the capping layer. It was reported that when aerated bubbles
316 are in nano size (<200 nm), they can have much longer life than the macro bubbles (Ebina et al.,
317 2013). These oxygen nanobubbles can slowly diffuse oxygen into the water column and maintain the
318 higher DO level (4-7.5 mg/L) in ONMZ and ONMS. The reversed ORP values from -200 mV to 180-

210 mV in ONMZ for 89 days indicated that oxidation status can be sustained in the capping layer for very long time beyond months. Part of oxygen nanobubbles can be generated and stable exist at the zeolite/soil particle-water interfaces in the experiment which can be inferred from the evidence that a stable cloud of $O_2$ nanobubbles could be found at the diatomite particle-water interface after oxygen loading (Pan et al., 2016). Oxygen retention in the capping layer and downward penetration of oxygen into the deeper sediment formed an oxygen-locking sediment layer and contribute to a persistent reversal of anoxic condition. The oxygen nanobubbles appeared to either be active or have provided sufficient oxidation to maintain elevated levels of DO and redox potential for 3-4 months in the present study. At the end of present study, it was visually evidenced that around 4 cm of sediment at the SWI showed a light yellow color in the ONMZ systems, which was in sharp contrast to an unchanged black anoxic layer in the control systems (Fig. 7).

Although the previous study shows that the chitosan modified soils could form a capping layer on the sediment to decrease the internal nutrients loading, the capper layer could not provide extra oxygen delivery into the water and sediment and thus only can remediate the hypoxia for a short period (Pan et al., 2012).The color difference of the sediment in the present study indicated that in addition to direct diffusion of oxygen into the water column, there was significant amount of oxygen loaded in ONMZ and ONMS that can penetrate into the sediment at a considerable depth. This likely facilitated oxidation of organic matter as well as reduced substances. What is most important is that such a layer provides physical isolation to prevent reduced substances from the anoxic layer from diffusing upwards into the water column. Most hypoxia is formed when DO in bottom water is consumed by the anaerobic substances from the sediment while there is not enough oxygen replenishing from the surface water. The reversal of ORP at SWI in the ONMZ and ONMS systems

(Fig. 3b) could be expected to lead to oxidation of reduced forms of iron, manganese, methyl-mercury and sulfide that would otherwise be released from the sediment (Beutel et al., 2008; De Vittor et al., 2016; Gantzer et al., 2009; Testa and Kemp, 2012; Zhu et al., 2013). The nanobubble technology demonstrated in this study appeared to provide a novel principle for the remediation of hypoxia/anoxia in the bottom water.

### 4.3 Manipulating nutrients fluxes at SWI

Reversal of hypoxia/anoxia may not only prevent the release of reduced species release and facilitate organic matter mineralization (Beutel et al., 2008; De Vittor et al., 2016; Gantzer et al., 2009; Testa and Kemp, 2012), but can also influence nutrient recycling across SWI. In the present study, evidence of the positive effect of alleviation of hypoxia remediation on nutrient recycling was found in the significant differences in nutrient concentrations and fluxes across SWI between the ONMZ and ONMS treated and control systems (**Error! Reference source not found.**4 and **Error! Reference source not found.**5). Obvious P release from the sediment to the overlying water occurred in the control system, however, there was a net flux of TP from water to the sediments in the ONMZ and ONMS systems (**Error! Reference source not found.**4b and **Error! Reference source not found.**5a). Although, in some previous reports, capping with unmodified materials could also influence nutrient fluxes in short period (Faithfull et al., 2008; Pan et al., 2012), no evidence showed these materials could reversal the sediment hypoxia/anoxia which can contribute to P fixation in sediment. The main mechanism of the P release from sediments is generally related to changes in redox-sensitive iron and manganese oxide minerals and the associated P (Funes et al., 2016; Jordan et al., 2008), with inorganic phosphorus generally adsorbed by the metal oxide–hydroxide complexes under oxic conditions (Tang et al., 2013; Xu et al., 2013). Reversal of the ORP sign (i.e., positive

values) in ONMZ treated systems indicated that the SWI changed from anoxic to oxic. Jilbert et al. (2011) found preferential remineralization of P in relation to carbon and nitrogen during decomposition of organic substances induced by reducing conditions plays a key role leading to surplus bioavailable P in the Baltic Sea, and was likely why TP concentrations in the overlying water were significantly positively correlated with DO and ORP (Table 1). Reversal of ORP in ONMZ induced a conversion of sediment from P sources to sinks compared with that in the control.

Changes in redox potential affect N transformations from bacterial activities at the SWI, particularly nitrification, denitrification and anammox reactions (Brzozowska and Gawronska, 2009). The significantly higher oxygen condition induced by surface oxygen nanobubble materials (**Error! Reference source not found.**3) may facilitate nitrification, which converts $NH_4^+$-N to $NO_3^-$-N (Rassamee et al., 2011). Thus, lower $NH_4^+$-N occurred in ONMZ. Moreover, nitrification can supply necessary $NO_2^-$-N as an electron acceptor to anammox bacteria which can reduce $NH_4^+$-N to nitrogen gas (Kim et al., 2016). Nitrification-anammox coupling reactions often occur between aerobic and anaerobic zones (Brzozowska and Gawronska, 2009), notably in the SWI region. The co-existence of nitrification and anammox in the treated systems may reduce the efflux of $NH_4^+$-N in the experimental systems compared with those in the control at the end of the experiment (**Error! Reference source not found.**5c). In control systems, anaerobic conditions not only hinder nitrification and supply of $NO_2^-$-N for anammox bacteria but may also stimulate sulfide accumulation, further inhibiting nitrification (Jensen et al., 2008). Thus, the lowest concentrations of $NO_3^-$-N in the control systems were likely to have been through denitrification (**Error! Reference source not found.**4e). Beyond denitrification, dissimilatory $NO_3^-$-N reduction to $NH_4^+$-N can also be facilitated under anoxic conditions (McCarthy et al., 2008). The sum of these effects contributed to the reduced

385 TN efflux in the treated systems (**Error! Reference source not found.**5b). It should be noted that
386 local soils, collected from the lake and used in our experiment, may contain more organic matter than
387 zeolite. The higher $NH_4^+$-N concentrations in the ONMS treated systems might be produced by
388 mineralization of organic N from the soils (**Error! Reference source not found.**4d). Previous studies
389 point out that organic matter in the anoxic sediment could be degraded together with N
390 transformations from organic N to $NH_4^+$-N within two weeks (Han et al., 2015; Xu et al., 2013). This
391 is consistent with our results that $NH_4^+$-N increased between 19 and 33 days and decreased in the
392 subsequent days in all the three systems (**Error! Reference source not found.**4d). As a result of
393 these processes above mentioned, using surface oxygen nanobubble technology can significantly
394 regulate the biogeochemical processes that regulate species of phosphorus and nitrogen at the SWI.
395 It would be an important topic to study the role of oxygen nanobubbles in relation to microbial
396 communities under controlled laboratory and field conditions.

397 **4.4 Implementation perspective for lake geo-engineering**

398 The present study has, for the first time, indicated that oxygen nanobubble modified clays can
399 deliver amounts of oxygen into both water and sediment where there has previously been
400 hypoxia/anoxia. By using the geo-engineering method developed based on oxygen nanobubbles, it is
401 possible to deliver oxygen into bottom water/sediment through gravity settling, which can achieve
402 both replenishing oxygen consumption in the "dead zone" with minimum energy consumption and
403 minimizing the disturbance to the water stratification and surface sediment. The prolonged time
404 effects of oxygen nanobubbles, denoted by improving oxygen levels and reversal of ORP, may further
405 trigger a series changes in physico-chemical and microbial responses at SWI. Nevertheless, the in-
406 site experiment of the surface nanobubble technology in lakes and sea waters need to be further

investigated.

## 5. Conclusions

The study verified a novel principle for combating hypoxia/anoxia at the sediment-water interfaces using oxygen nanobubble technology. The synergistic effects of diffusion and retention of oxygen in the nanobubble modified natural zeolite (ONMZ) and local soils (ONMS) contributed to mitigating sediment anoxia and controlling phosphorus release from bottom sediments. It was found that amount of oxygen loaded in clay particles could release via both macro- and nano-scale bubbles and quickly increase the DO levels in water column. Moreover, the oxygen nanobubbles in the modified particles could stably retain at SWI and penetrate oxygen downward to the sub-layer sediment, and then form an oxygen-locking sediment layer between the anoxic sediment and water column. This layer can sustainably reverse hypoxia/anoxia condition at SWI for several months. Finally, nutrient fluxes across the SWI could be regulated by capping with oxygen nanobubble modified materials in which the bottom sediments become adsorptive for phosphorus, rather than releasing it. In this study we have demonstrated the potential for a major breakthrough in remediation of aquatic systems via geo-engineering and delivery of oxygen and form oxygen-locking later into the deep sediment-water interface, which is crucial for eutrophication control and ecological restoration.

## Acknowledgments

The research was supported by the Strategic Priority Research Program of CAS (XDA09030203), National Natural Science Foundation of China (41401551), Beijing Natural Science Foundation (8162040) and National Key Research and Development Program of China

(2017YFA0207204). It was further supported by the Bay of Plenty Regional Council and the New Zealand Ministry of Business, Innovation and Employment (UOWX1503; Enhancing the health and resilience of New Zealand lakes).

## References


Agarwal A, Ng WJ, Liu Y, 2011. Principle and applications of microbubble and nanobubble technology for water treatment. Chemosphere 84 (9), 1175-1180.

APHA, 1998. Standard methods for the examination of water and wastewat. American Public Health Association, Washington DC 20th Edition.

Beutel MW, Horne AJ, 1999. A Review of the Effects of Hypolimnetic Oxygenation on Lake and Reservoir Water Quality. Lake Reservoir Manag. 15 (4), 285-297.

Beutel MW, Leonard TM, Dent SR, Moore BC, 2008. Effects of aerobic and anaerobic conditions on P, N, Fe, Mn, and Hg accumulation in waters overlaying profundal sediments of an oligo-mesotrophic lake. Water Res. 42 (8-9), 1953-1962.

Bierlein KA, Rezvani M, Socolofsky SA, Bryant LD, Wüest A, Little JC, 2017. Increased sediment oxygen flux in lakes and reservoirs: The impact of hypolimnetic oxygenation. Water Resources Research.

Bormans M, Marsalek B, Jancula D, 2016. Controlling internal phosphorus loading in lakes by physical methods to reduce cyanobacterial blooms: a review. Aquat. Ecol. 50 (3), 407-422.

Bryant LD, Lorrai C, McGinnis DF, Brand A, Wuest A, Little JC, 2010. Variable sediment oxygen uptake in response to dynamic forcing. Limnol. Oceanogr. 55 (2), 950-964.

Brzozowska R, Gawronska H, 2009. The influence of a long-term artificial aeration on the nitrogen compounds exchange between bottom sediments and water in Lake Dlugie. Oceanological and Hydrobiological Studies 38 (1), 113-119.

Cai WB, Yang HL, Zhang J, Yin JK, Yang YL, Yuan LJ, et al., 2015. The Optimized Fabrication of Nanobubbles as Ultrasound Contrast Agents for Tumor Imaging. Sci Rep-Uk 5, 13725.

454 Carstensen J, Andersen JH, Gustafsson BG, Conley DJ, 2014. Deoxygenation of the Baltic Sea during
455 the last century. Proc. Natl. Acad. Sci. U. S. A. 111 (15), 5628-5633.
456 Cavalli R, Bisazza A, Rolfo A, Balbis S, Madonnaripa D, Caniggia I, et al., 2009. Ultrasound-
457 mediated oxygen delivery from chitosan nanobubbles. Int. J. Pharm. 378 (1–2), 215-217.
458 Conley DJ, Bonsdorff E, Carstensen J, Destouni G, Gustafsson BG, Hansson LA, et al., 2009.
459 Tackling Hypoxia in the Baltic Sea: Is Engineering a Solution? Environ. Sci. Technol. 43 (10),
460 3407-3411.
461 De Vittor C, Relitti F, Kralj M, Covelli S, Emili A, 2016. Oxygen, carbon, and nutrient exchanges at
462 the sediment–water interface in the Mar Piccolo of Taranto (Ionian Sea, southern Italy). Environ.
463 Sci. Pollut. Res. 23 (13), 12566-12581.
464 Diaz RJ, Rosenberg R, 2008. Spreading dead zones and consequences for marine ecosystems. Science
465 321 (5891), 926-929.
466 Ebina K, Shi K, Hirao M, Hashimoto J, Kawato Y, Kaneshiro S, et al., 2013. Oxygen and Air
467 Nanobubble Water Solution Promote the Growth of Plants, Fishes, and Mice. PLoS One 8 (6).
468 Faithfull CL, Hamilton DP, Burger DF, Duggan IC. Waikato peat lakes sediment nutrient removal
469 scoping exercise. CBER Contract Report. The University of Waikato, 2008.
470 Feist TJ, Pauer JJ, Melendez W, Lehrter JC, DePetro PA, Rygwelski KR, et al., 2016. Modeling the
471 Relative Importance of Nutrient and Carbon Loads, Boundary Fluxes, and Sediment Fluxes on
472 Gulf of Mexico Hypoxia. Environ. Sci. Technol. 50 (16), 8713-8721.
473 Forth M, Liljebladh B, Stigebrandt A, Hall POJ, Treusch AH, 2015. Effects of ecological engineered
474 oxygenation on the bacterial community structure in an anoxic fjord in western Sweden. ISME J.
475 9 (3), 656-669.

476 Funes A, de Vicente J, Cruz-Pizarro L, Alvarez-Manzaneda I, de Vicente I, 2016. Magnetic
477 microparticles as a new tool for lake restoration: A microcosm experiment for evaluating the
478 impact on phosphorus fluxes and sedimentary phosphorus pools. Water Res. 89, 366-374.
479 Funkey CP, Conley DJ, Reuss NS, Humborg C, Jilbert T, Slomp CP, 2014. Hypoxia Sustains
480 Cyanobacteria Blooms in the Baltic Sea. Environ. Sci. Technol. 48 (5), 2598-2602.
481 Gachter R, Wehrli B, 1998. Ten years of artificial mixing and oxygenation: No effect on the internal
482 phosphorus loading of two eutrophic lakes. Environ. Sci. Technol. 32 (23), 3659-3665.
483 Gafsi M, Kettab A, Djehiche A, Goteicha K, 2016. Study of the efficiency of hypolimnetic aeration
484 process on the preservation of the thermal stratification. Desalin Water Treat 57 (13), 6017-6023.
485 Gantzer PA, Bryant LD, Little JC, 2009. Controlling soluble iron and manganese in a water-supply
486 reservoir using hypolimnetic oxygenation. Water Res. 43 (5), 1285-1294.
487 Han C, Ding SM, Yao L, Shen QS, Zhu CG, Wang Y, et al., 2015. Dynamics of phosphorus-iron-
488 sulfur at the sediment-water interface influenced by algae blooms decomposition. J. Hazard.
489 Mater. 300, 329-337.
490 Henares MNP, Preto BD, Rosa FRT, Valenti WC, Camargo AFM, 2015. Effects of artificial substrate
491 and night-time aeration on the water quality in Macrobrachium amazonicum (Heller 1862) pond
492 culture. Aquac. Res. 46 (3), 618-625.
493 Huser BJ, Futter M, Lee JT, Perniel M, 2016. In-lake measures for phosphorus control: The most
494 feasible and cost-effective solution for long-term management of water quality in urban lakes.
495 Water Res. 97, 142-152.
496 Jensen MM, Kuypers MMM, Lavik G, Thamdrup B, 2008. Rates and regulation of anaerobic
497 ammonium oxidation and denitrification in the Black Sea. Limnol. Oceanogr. 53 (1), 23-36.

498 Jilbert T, Slomp CP, Gustafsson BG, Boer W, 2011. Beyond the Fe-P-redox connection: preferential
499 regeneration of phosphorus from organic matter as a key control on Baltic Sea nutrient cycles.
500 Biogeosciences 8 (6), 1699-1720.
501 Jordan TE, Cornwell JC, Boynton WR, Anderson JT, 2008. Changes in phosphorus biogeochemistry
502 along an estuarine salinity gradient: The iron conveyer belt. Limnol. Oceanogr. 53 (1), 172-184.
503 Kim H, Ogram A, Bae H-S, 2016. Nitrification, Anammox and Denitrification along a Nutrient
504 Gradient in the Florida Everglades. Wetlands, 1-9.
505 Li L, Pan G, 2013. A universal method for flocculating harmful algal blooms in marine and fresh
506 waters using modified sand. Environ. Sci. Technol. 47 (9), 4555-4562.
507 Liboriussen L, Sondergaard M, Jeppesen E, Thorsgaard I, Grunfeld S, Jakobsen TS, et al., 2009.
508 Effects of hypolimnetic oxygenation on water quality: results from five Danish lakes.
509 Hydrobiologia 625, 157-172.
510 McCarthy MJ, McNeal KS, Morse JW, Gardner WS, 2008. Bottom-water hypoxia effects on
511 sediment-water interface nitrogen transformations in a seasonally hypoxic, shallow bay (Corpus
512 christi bay, TX, USA). Estuaries and Coasts 31 (3), 521-531.
513 Noyma NP, de Magalhães L, Furtado LL, Mucci M, van Oosterhout F, Huszar VLM, et al., 2016.
514 Controlling cyanobacterial blooms through effective flocculation and sedimentation with
515 combined use of flocculants and phosphorus adsorbing natural soil and modified clay. Water Res.
516 97, 26-38.
517 Pan G, Dai LC, Li L, He LC, Li H, Bi L, et al., 2012. Reducing the Recruitment of Sedimented Algae
518 and Nutrient Release into the Overlying Water Using Modified Soil/Sand Flocculation-Capping
519 in Eutrophic Lakes. Environ. Sci. Technol. 46 (9), 5077-5084.

520 Pan G, He G, Zhang M, Zhou Q, Tyliszczak T, Tai R, et al., 2016. Nanobubbles at Hydrophilic
521 Particle-Water Interfaces. Langmuir 32 (43), 11133-11137.
522 Pan G, Krom MD, Zhang MY, Zhang XW, Wang LJ, Dai LC, et al., 2013. Impact of Suspended
523 Inorganic Particles on Phosphorus Cycling in the Yellow River (China). Environ. Sci. Technol.
524 47 (17), 9685-9692.
525 Pan G, Yang B, 2012. Effect of Surface Hydrophobicity on the Formation and Stability of Oxygen
526 Nanobubbles. Chemphyschem 13 (8), 2205-2212.
527 Pan G, Yang B, Lei L, Lei, Liao L, Ding C, Wang D, 2011. A method for remediating of anoxic
528 sediment in lakes by using nanobubbles. Patent NO. 200910080563.5.
529 Peng H, Birkett GR, Nguyen AV, 2015. Progress on the Surface Nanobubble Story: What is in the
530 bubble? Why does it exist? Adv. Colloid Interface Sci. 222, 573-580.
531 Rassamee V, Sattayatewa C, Pagilla K, Chandran K, 2011. Effect of Oxic and Anoxic Conditions on
532 Nitrous Oxide Emissions from Nitrification and Denitrification Processes. Biotechnol. Bioeng.
533 108 (9), 2036-2045.
534 Spears BM, Maberly SC, Pan G, Mackay E, Bruere A, Corker N, et al., 2014. Geo-Engineering in
535 Lakes: A Crisis of Confidence? Environ. Sci. Technol. 48 (17), 9977-9979.
536 Stigebrandt A, Gustafsson BG, 2007. Improvement of Baltic proper water quality using large-scale
537 ecological engineering. Ambio 36 (2-3), 280-286.
538 Stramma L, Johnson GC, Sprintall J, Mohrholz V, 2008. Expanding oxygen-minimum zones in the
539 tropical oceans. Science 320 (5876), 655-658.
540 Tang WZ, Zhang H, Zhang WQ, Wang C, Shan BQ, 2013. Biological invasions induced phosphorus
541 release from sediments in freshwater ecosystems. Colloid Surface A 436, 873-880.

542 Testa JM, Kemp WM, 2012. Hypoxia-induced shifts in nitrogen and phosphorus cycling in
543 Chesapeake Bay. Limnol. Oceanogr. 57 (3), 835-850.
544 Waajen G, van Oosterhout F, Douglas G, Lürling M, 2016. Geo-engineering experiments in two
545 urban ponds to control eutrophication. Water Res. 97, 69-82.
546 Wang L, Miao XJ, Pan G, 2016. Microwave-Induced Interfacial Nanobubbles. Langmuir 32 (43),
547 11147-11154.
548 Xu D, Chen YF, Ding SM, Sun Q, Wang Y, Zhang CS, 2013. Diffusive Gradients in Thin Films
549 Technique Equipped with a Mixed Binding Gel for Simultaneous Measurements of Dissolved
550 Reactive Phosphorus and Dissolved Iron. Environ. Sci. Technol. 47 (18), 10477-10484.
551 Yang CW, Lu YH, Hwang IS, 2013. Condensation of Dissolved Gas Molecules at a
552 Hydrophobic/Water Interface. Chinese J Phys 51 (1), 174-186.
553 Zhang ZS, Wang G, Li Y, Zhang X, Qiao NL, Wang JH, et al., 2014. A new type of ordered
554 mesoporous carbon/polyaniline composites prepared by a two-step nanocasting method for high
555 performance supercapacitor applications. J Mater Chem A 2 (39), 16715-16722.
556 Zhu G, Wang S, Wang W, Wang Y, Zhou L, Jiang B, et al., 2013. Hotspots of anaerobic ammonium
557 oxidation at land-freshwater interfaces. Nature Geosci 6 (2), 103-107.
558
559
560